Society of Medical Education & Research

2026, Volume 6, Issue 1, Page No: 130-140
ISSN: 3108-4834

Archive of International Journal of Cancer and Allied Science

Immune Checkpoint Dysregulation in Epidermolysis Bullosa-Associated Squamous Cell Carcinomas Reveals an Immunosuppressive Tumor Microenvironment

Lina Hassan[1]*, Omar Khalaf[2], Reem Jaber[1], Rania Mostafa[3]

[1]Department of Rare Tumor Biology and EB-Associated SCC, Faculty of Medicine, University of Jordan, Amman, Jordan.
[2]Department of Immune Checkpoint Dysregulation and TME, Faculty of Medicine, Jordan University of Science and Technology, Irbid, Jordan.
[3]Department of Immunosuppressive Tumor Microenvironment, Faculty of Medicine, Al-Balqa Applied University, Salt, Jordan.

***E-mail** ✉ lina.hassan@ju.edu.jo

Abstract

Cutaneous squamous cell carcinomas (SCCs) emerge as a serious sequela in selected forms of epidermolysis bullosa (EB), carrying elevated risks of morbidity and mortality along with considerable gaps in effective management strategies. Elevated endogenous mutagenesis coupled with a desmoplastic stromal reaction is implicated in disease development. Individuals with dystrophic EB (DEB) and Kindler EB (KEB) are most at risk of SCC formation. A parallel high-risk cohort includes immunosuppressed (IS) patients, notably organ transplant recipients. This work explores potential dysregulation of immune checkpoint proteins and suppressive enzymes in EB-related SCCs to evade host immunity. Expression profiles are contrasted with those detected in SCCs from IS patients—who commonly manifest aggressive lesions—as well as sporadic tumors in immunocompetent (IC) subjects. Immunohistochemistry coupled with semi-quantitative scoring was employed to assess indoleamine 2,3-dioxygenase (IDO), programmed cell death protein-1 (PD-1), programmed cell death ligand-1 (PD-L1), T cell immunoglobulin and mucin-domain-containing protein-3 (TIM-3), lymphocyte activation gene-3 (LAG-3), and key inflammatory populations (CD4, CD8, and CD68) in cohorts comprising 30 DEB-SCCs, 22 KEB-SCCs, 106 IS-SCCs, and 100 IC-SCCs. DEB-SCCs exhibited markedly elevated IDO and PD-L1 within carcinoma cells and increased PD-1 in the tumor microenvironment (TME) relative to both IC-SCCs and IS-SCCs. CD4-positive T-cell density per mm² proved significantly diminished in DEB-SCCs compared with IC-SCCs. KEB-SCCs displayed minimal expression of the T-cell exhaustion markers TIM-3 and LAG-3 across all evaluated groups. Collectively, these observations highlight IDO, PD-1, and PD-L1 as upregulated in EB-SCCs and warrant consideration as candidates for combined therapeutic approaches, particularly in DEB-SCC cases.

Keywords: Epidermolysis bullosa, Collagen VII, Kindlin, Squamous cell carcinoma, Indoleamine 2,3-dioxygenase, Programmed cell death protein-1

Introduction

Particular variants of epidermolysis bullosa (EB) confer heightened susceptibility to squamous cell carcinomas (SCCs) developing at sites of persistent cutaneous and mucosal injury [1-3]. Both dystrophic EB (DEB) and Kindler EB (KEB) are linked to recurrent SCCs that present early in life, demonstrate prompt metastatic dissemination, and pursue an aggressive, life-threatening trajectory [4-7]. SCCs in DEB have been recorded in patients as young as 13 years, often associated with poor survival [8]. In KEB, tumors preferentially arise in zones subjected to intense ultraviolet radiation or repeated mechanical trauma [4, 6, 9]. The earliest documented KEB-associated SCC (KEB-SCC) occurred in a 6-year-old child [10]. Surgical resection with wide margins or

Access this article online https://smerpub.com/

Received: 08 January 2026; **Accepted:** 16 April 2026

How to cite this article: Hassan L, Khalaf O, Jaber R, Mostafa R. Immune Checkpoint Dysregulation in Epidermolysis Bullosa-Associated Squamous Cell Carcinomas Reveals an Immunosuppressive Tumor Microenvironment. Arch Int J Cancer Allied Sci. 2026;6(1):130-40. https://doi.org/10.51847/rJ1vtTh4a1

amputation currently represents the mainstay of management [4]. Insights into the efficacy of immunotherapy for advanced EB-SCC derive predominantly from isolated case reports and modest patient series [4, 11-19]. This population therefore faces a pressing need for improved treatment options.

Within DEB skin, intrinsic mutational signatures driven primarily by apolipoprotein B mRNA-editing enzyme, catalytic polypeptide-like (APOBEC) activity result in extensive early mutational accumulation [20]. Ongoing cellular stress and inflammatory signals stemming from recurrent wounding and microbial exposure activate APOBEC pathways [20]. Mutational characteristics of KEB-SCC have yet to be delineated. Nevertheless, kindlin-1 modulates cell-cycle checkpoints and genomic integrity [21] and contributes to the biology of multiple tumor types [22-25].

Activation of fibroblasts, transforming growth factor beta-1 cascades, and related reparative signaling networks feature prominently in both DEB and KEB [26-32]. The resulting fibrotic microenvironment is considered a key driver of the aggressive phenotype of DEB-SCC. Inflammatory processes in EB involve intricate interactions between wound-healing responses and bacterial colonization, both of which potentiate malignant transformation [33]. Emerging laboratory findings suggest that PD-1/Treg-dependent mechanisms may restrain adaptive T-cell responses in DEB [34]. Despite these observations, detailed characterization of the immune contexture in EB-SCC remains sparse.

Enhanced expression of immune checkpoint components on neoplastic cells and associated stromal populations can markedly impair effective antitumor immunity. Key regulators such as programmed cell death protein-1 (PD-1) on T lymphocytes and programmed cell death ligand-1 (PD-L1) on tumor or antigen-presenting cells critically influence tumor monitoring; therapeutic blockade of this axis augments T-cell effector functions [35, 36]. Indoleamine 2,3-dioxygenase (IDO) catalyzes the conversion of L-tryptophan to kynurenine, thereby establishing an immunosuppressive niche that favors regulatory T-cell expansion [37, 38]. Additional exhaustion markers on T cells, including T cell immunoglobulin and mucin-domain-containing protein-3 (TIM-3) and lymphocyte activation gene-3 (LAG-3), represent further actionable targets capable of restoring T-cell competence and promoting tumor clearance [39, 40].

The principal objective of this study was to ascertain whether EB-SCCs display altered immune checkpoint profiles that may explain their unfavorable prognosis and offer opportunities for targeted intervention.

Materials and Methods

Patients and samples

The investigation encompassed 258 cutaneous SCC specimens. These included 30 tumors from patients with recessive DEB (n = 9), 22 tumors from individuals with KEB (n = 7), 100 sporadic SCCs originating on sun-exposed areas in immunocompetent subjects (IC-SCCs) (n = 96), and 106 tumors resected from immunosuppressed patients (IS-SCCs) (n = 41) **(Table 1)**. EB patients had not been exposed to anti-proliferative agents, immunotherapy, or radiation therapy before tumor removal, apart from one case (DEB-P1), who had undergone prior anti-PD-1 treatment before resection of a right-hand lesion [15]. Immunosuppressed participants presented with conditions such as organ or stem cell transplantation, autoimmune inflammatory disorders, primary immunodeficiency, solid neoplasms, or blood cancers. All lesions were surgically removed for clinical indications. Tumor morphology was documented from original pathology reports, with corresponding hematoxylin and eosin (H&E) slides re-examined for confirmation. Ethical approval was granted by the University of Freiburg Ethics Committee (EK-Freiburg 45/18 and 5/20), and the work adhered to the Declaration of Helsinki guidelines.

Table 1. Patient and tumor clinicopathological features.

Characteristic	IS-SCC[4]	IC-SCC[3]	KEB-SCC[2]	DEB-SCC[1]
Number of patients / SCC samples	41 / 106	96 / 100	7 / 22	9 / 30
Mean age at SCC diagnosis, years (range)	68 (41–87)	80 (45–99)	47 (30–65)	32 (18–50)
Sex distribution (male: female)	27:14	58:38	5:2	4:5
Tumor localization, n (%)				
Head and neck	54 (51)	79 (79)	7 (32)	0 (0)
Trunk	17 (16)	0 (0)	0 (0)	0 (0)
Upper extremities	24 (23)	19 (19)	5 (23)	16 (53)
Lower extremities	11 (10)	2 (2)	10 (45)	14 (47)
Histological grade, n (%)				
G1	38 (36)	48 (48)	8 (36)	22 (73)
G2	60 (57)	51 (51)	3 (14)	5 (17)
G3	8 (7)	1 (1)	11 (50)	3 (10)
Vertical tumor thickness, n (%)				
≤2 mm	35 (33)	42 (42)	6 (27)	7 (23)

2.01–6 mm	58 (55)	40 (40)	16 (73)	14 (47)
>6 mm	9 (8)	18 (18)	0 (0)	5 (17)
Not available (NA)	4 (4)	0 (0)	4 (13)	6

[1] Recessive dystrophic EB; [2] squamous cell carcinoma; [3] Kindler EB; [4] immunocompetent; [5] immunosuppressed; [6] not available.

Immunohistochemistry

Five-micrometer serial sections were generated from formalin-fixed paraffin-embedded tissue blocks. Conventional hematoxylin and eosin staining supported routine diagnostic evaluation. Immunohistochemical (IHC) procedures involved deparaffinization and heat-induced epitope retrieval with either EDTA (pH 9) or citrate (pH 6) buffers. Selected slides received a pre-incubation step in blocking buffer (2% BSA + 0.05% Tween 20 in TBS) for 30 min at room temperature to reduce non-specific labeling. All antibodies were prepared in commercial diluent (Zytomed; catalog number: ZUC025). Primary antibody incubation lasted 60 min at room temperature. Negative controls consisted of sections exposed only to secondary reagents. Immunoreactivity was visualized with the Dako REAL™ alkaline phosphatase/RED detection kit for rabbit/mouse antibodies (Dako, catalog number: K5005). Microscopic images were acquired on a Zeiss Axioscope (Carl Zeiss, Jena, Germany) and documented using AxioVision software (Carl Zeiss, Jena, Germany, SE64 release 4.9).

H-scores for IDO, PD-1, PD-L1, TIM-3, and LAG-3 were computed semiquantitatively via the equation: H-score = [1 × (% cells 1+) + 2 × (% cells 2+) + 3 × (% cells 3+)]. Membrane staining intensity was categorized as 0 = negative, 1+ = faint, 2+ = intermediate, or 3+ = intense [8]. Three independent evaluators, unaware of clinical details, performed the scoring.

Densities of CD4+, CD8+, and CD68+ cells were quantified as cells per mm² with QuPath software (Version 0.4.1) [41]. Mean values were obtained from a minimum of three representative tumor fields at ×10 magnification using automated positive cell identification and tallying functions.

Statistical analysis

Marker expression was analyzed within each SCC category and referenced against the IC-SCC group. Figures and statistical evaluations were produced in GraphPad Prism version 9.4.1 (GraphPad Software, La Jolla, CA, USA, www.graphpad.com, accessed on 13 January 2024)—inter-group comparisons utilized Kruskal–Wallis testing with Dunn's post-hoc correction. Linear regression was used to assess potential relationships between tumor depth and H-score values. A threshold of $p < 0.05$ indicated statistical significance.

Results and Discussion

Clinicopathological characteristics of SCCs

Clinicopathological details regarding the participants and their tumors are presented in **Table 1**. Typical clinical appearances of SCCs from the various subgroups are illustrated in **Figure 1**. The average age at tumor diagnosis was 32 years among DEB patients (range: 18–50), 47 years among KEB patients (range: 30–65), 80 years among IC patients (range: 45–99), and 68 years among IS patients (range: 41–87). DEB- and KEB-associated SCCs occurred predominantly on the extremities (100% and 68% of cases, respectively), whereas IC- and IS-SCCs were primarily found in the head and neck area (79% and 51%, respectively) **(Table 1)**. Fifty percent of the examined tumors displayed vertical thickness ranging from 2.01 to 6 mm. Lesions classified as high-risk due to thickness exceeding 6 mm comprised 17% of DEB-SCCs, 0% of KEB-SCCs, 18% of IC-SCCs, and 8% of IS-SCCs. Assessment of vertical thickness was not feasible in four DEB-SCCs and four IS-SCCs owing to specimen fragmentation. The IS-SCC cohort consisted of tumors from 34 organ transplant recipients (22 kidney, 1 liver, 2 lung, 1 heart, and 8 stem cell transplants), 4 patients managed for inflammatory or autoimmune conditions (two rheumatoid arthritis, one psoriasis, one bullous pemphigoid), 1 case of congenital immunodeficiency featuring CD4+ T-cell impairment, and 1 individual with treated B-CLL. Immunosuppressive agents administered included mTOR inhibitors (n = 5), calcineurin inhibitors (n = 24), purine synthesis inhibitors (n = 25), antimetabolites (n = 3), alkylating or alkylating-like agents (n = 2), and proteasome inhibitors (n = 1), with 23 patients receiving combined regimens.

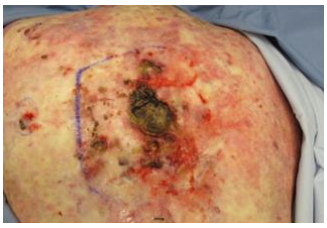

a)

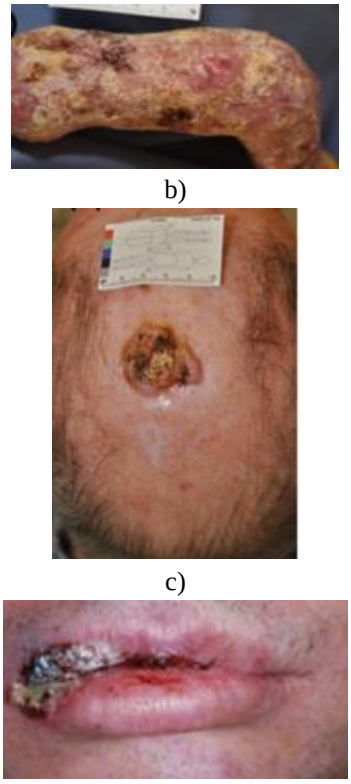

b)

c)

d)

Figure 1. Clinical manifestations of cutaneous SCCs in the different study populations

(a) SCC located on the back of an organ transplant recipient receiving dual immunosuppressive treatment, with surrounding poikilodermatous skin changes secondary to marked actinic damage, (b) Multiple SCCs affecting the severely deformed hand of a dystrophic EB patient, (c) SCC on the upper lip of a patient diagnosed with Kindler EB, and (d) Hyperkeratotic SCC on the scalp in an immunocompetent subject. EB, epidermolysis bullosa; SCC, squamous cell carcinoma.

DEB-SCC tumor cells express significantly higher levels of IDO and PD-L1 compared with IC- and IS-SCC tumor cells

Expression of IDO within carcinoma cells was substantially greater in DEB-SCCs (mean H-score: 48.32) than in KEB-SCCs (mean H-score: 10.8; P = 0.0038), IC-SCCs (mean H-score: 15.34; P < 0.0001), and IS-SCCs (mean H-score: 6.585; P < 0.0001) **(Figure 2)**. Expression levels did not differ meaningfully between IC-SCCs and IS-SCCs (mean H-scores: 15.34 versus 6.585) **(Figure 2)**. Similarly, PD-L1 staining intensity in DEB-SCC tumor cells exceeded that observed in IC-SCCs and IS-SCCs (mean H-scores: DEB—96.59 versus IC—26.36 versus IS—33.26; P < 0.0001 and P = 0.0021, respectively). KEB tumor cells also showed elevated PD-L1 compared with both control groups (mean H-scores: KEB—62.39 versus IC—26.36 versus IS—33.26; P = 0.0015 and P = 0.0304, respectively). Notably, tumor cells in both IC-SCCs and IS-SCCs displayed comparably negligible levels of IDO and PD-L1 **(Figure 2)**.

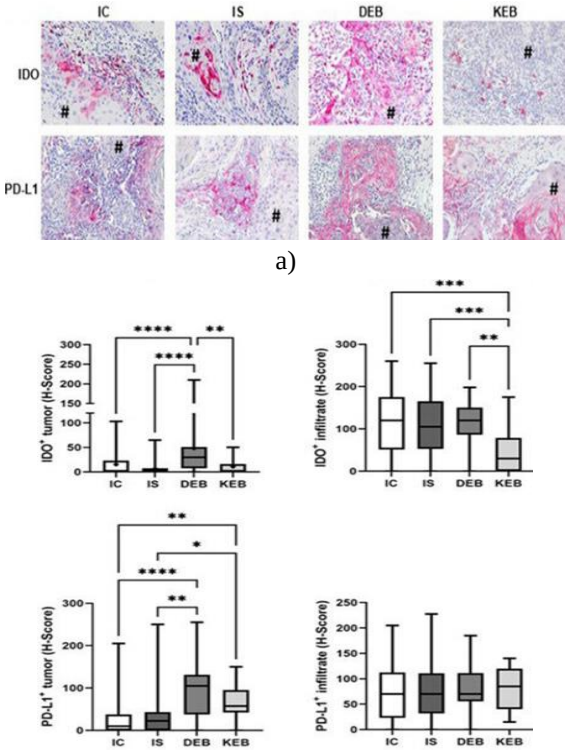

a)

b)

Figure 2. Expression of IDO and PD-L1 in cutaneous SCCs along with their tumor microenvironments

(a) Illustrative immunohistochemical (IHC) images from representative cases in each SCC category demonstrating IDO and PD-L1 localization in neoplastic cells and adjacent microenvironmental elements. # denotes tumor cells. Magnification = 200× and (b) Quantitative comparison of average IDO and PD-L1 expression across the SCC cohorts, measured by H-scores. IC = immunocompetent, IS = immunosuppressed, DEB = dystrophic EB, and KEB = Kindler EB. Asterisks indicate statistical significance: *P < 0.05; **P < 0.01; ***P < 0.001; ****P < 0.0001.

Analysis of the tumor microenvironment (TME) revealed broadly high IDO expression in non-tumor cells that was comparable across most subgroups (DEB-SCC

mean H-score: 108.1; IS-SCC mean H-score: 112.0; IC-SCC mean H-score: 114.4), except for significantly lower levels in KEB-SCCs (mean H-score: 46.14) **(Figure 2)**. PD-L1 expression in the TME showed no substantial variation among the four groups (mean H-scores: DEB-SCC—75.73, IS-SCC—76.86, IC-SCC—73.57, KEB—81.11) **(Figure 2)**. In aggregate, these data indicate that DEB-SCC tumor cells strongly induce IDO and PD-L1, thereby promoting immune resistance mechanisms that likely facilitate tumor establishment and progression.

The TME inflammatory cell infiltrate in EB-SCCs

Quantification of key inflammatory populations—CD4+ and CD8+ T cells, together with CD68+ macrophages—was performed in the TME of 25–30% of samples from each SCC category due to constraints on tissue availability **(Figure 3)**. DEB-SCCs contained markedly fewer CD4+ T cells (mean: 649 cells/mm²) compared with IC-SCCs (mean: 1211 cells/mm²; P = 0.0039), while a similar but non-significant decrease was noted versus IS-SCCs (mean: 1067 cells/mm²; P = 0.2084) **(Figure 3)**. The IS-SCC group exhibited the lowest CD8+ T-cell infiltration (mean: 692/mm²), which was significantly lower than in IC-SCCs (P = 0.0163). DEB-SCCs displayed a parallel downward trend (mean: 794/mm² versus IC mean: 1228/mm²; P = 0.1501) **(Figure 3)**. Macrophage (CD68+) numbers were significantly reduced in KEB-SCCs compared with IC-SCCs (mean: 338 cells/mm² versus 703 cells/mm²; P = 0.0113), whereas densities remained equivalent among DEB-, IC-, and IS-SCCs **(Figure 3)**. Overall, the TMEs of DEB- and IS-SCCs were marked by attenuated inflammatory infiltrates, particularly a paucity of tumor-infiltrating lymphocytes (TILs).

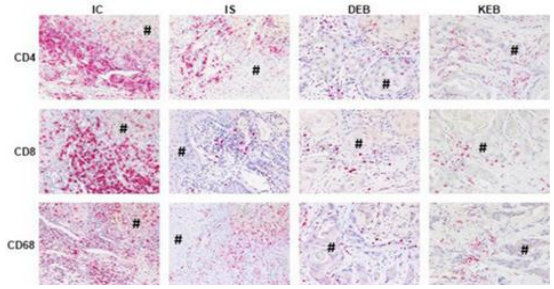

a)

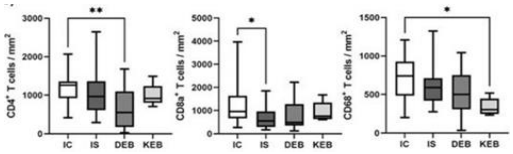

b)

Figure 3. Inflammatory cell populations within the TMEs of cutaneous SCCs

(a) Representative immunohistochemical staining images highlighting CD4+ and CD8+ T lymphocytes as well as CD68+ macrophages in the tumor microenvironment for each SCC category. # denotes tumor cells. Magnification = 200×, and (b) Quantitative comparison of mean absolute cell counts per mm² for CD4+, CD8+, and CD68+ populations across all SCC groups. IC = immunocompetent, IS = immunosuppressed, DEB = dystrophic EB, and KEB = Kindler EB. Asterisks denote statistical significance: *P < 0.05 and **P < 0.01.

PD-1 expression was significantly upregulated in the TMEs of DEB-, KEB-, and IS-SCCs, while LAG-3 was increased in the TME of IS-SCCs

Detailed examination of T-cell populations in the tumor microenvironment (TME) included evaluation of the checkpoint receptors PD-1, TIM-3, and LAG-3 **(Figure 4)**. PD-1 levels within the TME were notably elevated in DEB-SCCs (mean H-score: 151.8), KEB-SCCs (mean H-score: 132.1), and IS-SCCs (mean H-score: 118.6) when compared to IC-SCCs (mean H-score: 85.34; P < 0.0001, P = 0.0439, and P = 0.0057, respectively). DEB-SCCs displayed a tendency toward even greater PD-1 expression than IS-SCCs (mean H-score: 151.8 versus 118.6; P = 0.1513), though this comparison fell short of statistical significance **(Figures 4a and 4b)**. TIM-3 expression remained comparably strong in IC-SCCs (mean H-score: 69.13), IS-SCCs (mean H-score: 75.01), and DEB-SCCs (mean H-score: 86.57), but was markedly reduced in KEB-SCCs (mean H-score: 25.93) **(Figures 4a and 4b)**. In contrast, LAG-3 showed significantly higher expression in the TME of IS-SCCs (mean H-score: 53.07) relative to IC-SCCs (mean H-score: 31.68; P < 0.0001) and KEB-SCCs (mean H-score: 1.875; P < 0.0001) **(Figures 4a and 4b)**. Levels in IS-SCCs trended higher than in DEB-SCCs (mean H-score: 38.09; P = 0.1366) without reaching significance. KEB-SCCs exhibited significantly lower LAG-3 than DEB-SCCs (mean H-scores: 1.875 versus 38.09; P =

0.0138). Overall, PD-1 upregulation characterized the TME in EB-associated SCCs, while LAG-3 elevation was prominent in IS-SCCs.

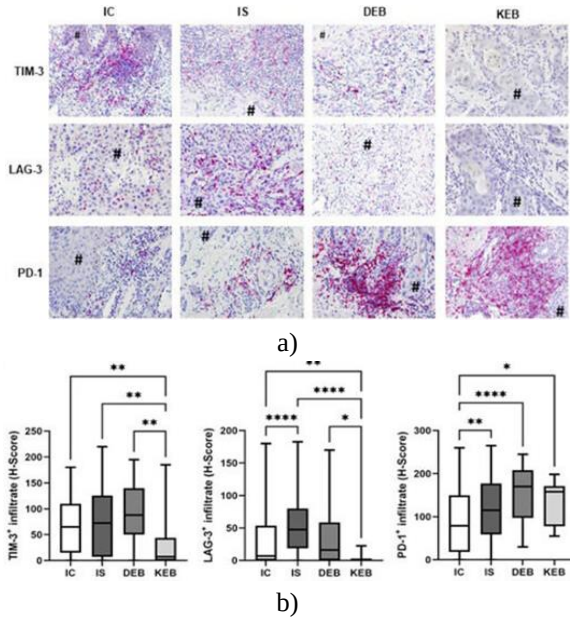

Figure 4. TIM-3, LAG-3, and PD-1 expression patterns in the TME of cutaneous SCCs

(a) Illustrative immunohistochemical images from each SCC category highlighting TIM-3, LAG-3, and PD-1 staining in stromal elements of the tumor microenvironment. # indicates tumor cells. Magnification = 200×, and (b) Quantitative assessment of average TIM-3, LAG-3, and PD-1 expression levels across SCC groups using H-scores. IC = immunocompetent, IS = immunosuppressed, DEB = dystrophic EB, and KEB = Kindler EB. Statistical significance levels are indicated as * P < 0.05), ** P < 0.01), and *** P < 0.0001).

Correlations between immune markers and clinicopathological parameters

The study investigated possible links between IDO and PD-L1 expression in carcinoma cells and vertical tumor thickness in EB-SCCs, considering the known association between greater depth and heightened metastatic potential [42] **(Figure 5)**. In IC-SCCs, IDO levels in tumor cells correlated strongly with vertical thickness (P < 0.004) **(Figure 5)**. No significant associations were detected in DEB-SCCs (P = 0.4047) or KEB-SCCs (P = 0.1194). PD-L1 expression in tumor cells correlated with thickness in IC-SCCs (P < 0.0038) and IS-SCCs (P = 0.0278) **(Figure 5)**. Within EB cases, a significant correlation appeared only in KEB-SCCs (P = 0.0013), but not in DEB-SCCs (P = 0.2125). Several thin DEB-SCCs nevertheless showed high IDO and PD-L1 levels, which may underlie the lack of correlation with depth in this subgroup. These findings suggest that IDO and PD-L1 expression in neoplastic cells may serve as surrogate prognostic indicators, particularly in IC- and IS-SCCs.

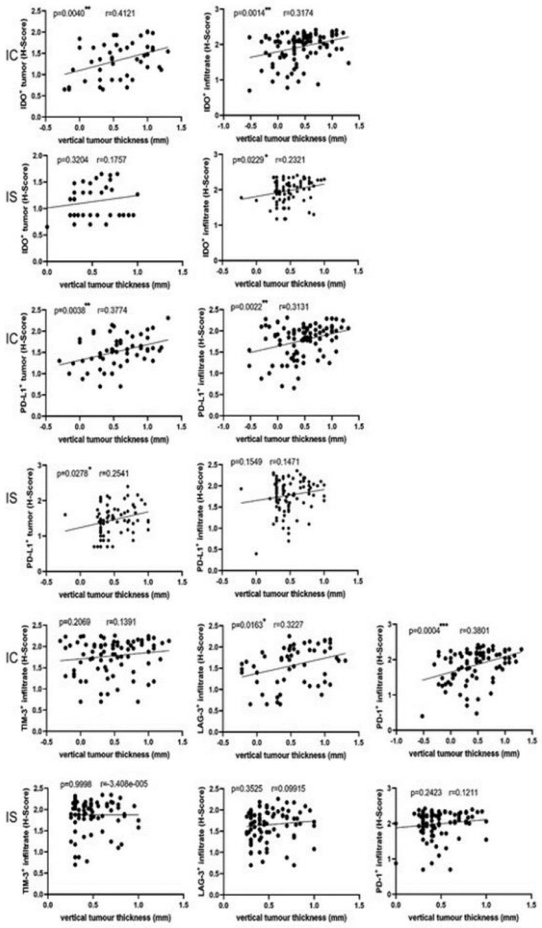

Figure 5. Relationship between immune marker levels and vertical tumor thickness.

Linear regression analysis depicting the influence of vertical tumor thickness (x-axis) on marker expression (y-axis) in both tumor cells and stromal compartments. IC = immunocompetent, IS = immunosuppressed. Significance is shown as * P < 0.05, ** P < 0.01, *** P < 0.001. r = Pearson correlation coefficient. Logarithmic transformation was applied to values on both axes before statistical testing.

Comparable associations were identified for IDO in TME cells, revealing significant correlations with vertical thickness in IC-SCCs (P = 0.0014) and IS-SCCs

(P = 0.0229) **(Figure 5)**, but none in DEB-SCCs (P = 0.6683) or KEB-SCCs (P = 0.6377). PD-L1 expression in the TME correlated robustly with tumor depth in IC-SCCs (P = 0.0022) **(Figure 5)**, with non-significant trends observed in IS-SCCs (P = 0.1549), DEB-SCCs (P = 0.0637), and KEB cases (P = 0.1475) **(Figure 5)**. Associations involving TME markers were therefore less consistent than those in tumor cells. Strong correlations in IC-SCCs nonetheless imply potential prognostic utility. Tumor grade correlations were additionally assessed, though limited by small numbers of higher-grade EB-SCCs and an absence of grade III/IV tumors in the IC group. Significant grade-related associations in IC-SCCs involved LAG-3 (P < 0.0163), TIM-3 (P = 0.014), tumor cell PD-L1 (P < 0.0001), and PD-1 (P = 0.029), with no corresponding findings in EB-SCCs or IS-SCCs.

Further evaluation of TME checkpoint molecules showed that LAG-3 and PD-1 expression in IC-SCCs correlated significantly with Breslow thickness (P = 0.0163 and P = 0.0004, respectively) **(Figure 5)**. No such relationships were present in IS-SCCs, DEB-SCCs, or KEB-SCCs **(Figure 5)**. In conclusion, heightened checkpoint expression on T cells within the TME, particularly in IC-SCCs, aligns with increased tumor thickness and may forecast unfavorable outcomes.

The influence of multi-agent immunosuppressive regimens on vertical tumor thickness and tumor aggressiveness was also explored in the IS-SCC cohort. No association was identified between the specific immunosuppressive agents employed, their number, or vertical tumor depth.

Interpretation of findings

Elucidating the mechanisms by which cancer cells evade immune detection through molecular camouflage is a central concern in cancer biology and underpins the development of novel therapeutic approaches. This investigation characterized the expression profiles of multiple immune checkpoint molecules in squamous cell carcinomas (SCCs) arising in patients with epidermolysis bullosa (EB), compared with those from immunocompetent and immunosuppressed individuals. SCCs in these cohorts emerged under markedly different conditions: (i) during youth in the context of chronically injured skin in EB; (ii) later in life among immunosuppressed hosts; or (iii) as UV-driven malignancies in elderly immunocompetent persons. Although the sample size of EB-SCCs is modest, it carries substantial weight for such an ultra-rare condition and aligns meaningfully with data from comparable research.

A key observation was the prominent expression of immunosuppressive checkpoint proteins by tumor cells in EB-SCCs. Persistent inflammation, ongoing tissue injury, extracellular matrix reorganization, and recurrent bacterial insults [43, 44] likely drive the induction of these molecules, allowing tumors to circumvent immune defenses at early stages and promote oncogenesis and advancement. DEB-SCCs displayed strong PD-L1 and IDO positivity in neoplastic cells, alongside PD-1 in the tumor microenvironment (TME), irrespective of lesion thickness. KEB-SCCs similarly demonstrated robust PD-L1 expression on tumor cells and PD-1 within the TME. PD-L1 upregulation may be mediated by transcription factors such as STAT3 or inflammatory cytokines including IFN, TNF, and IL-17, which are known to be elevated in DEB [45-47]. Tumor-derived IDO contributes to the creation of an immunosuppressive niche; notably, higher IDO levels in cutaneous melanoma have been associated with poorer progression-free survival. Phase II studies combining PD-1 blockade with IDO inhibition yielded favorable outcomes, with an objective response rate (ORR) of 51%, complete responses in 20% of cases, and disease control in 70% [48]. A separate phase I/II evaluation of an IDO/PD-L1-targeted vaccine plus nivolumab reported an ORR of 80% and complete responses in 43% of patients with metastatic melanoma [49].

DEB-SCCs contained fewer CD4+ cells in the TME than IC-SCCs. This is consistent with prior observations of markedly reduced peritumoral CD4+ infiltration in DEB-SCCs versus UV-induced SCCs, while levels were comparable to those in IS-SCCs [50, 51]. Elevated baseline TIL density has been linked to superior clinical outcomes in various solid tumors treated with immune checkpoint therapy [52]. CD8+ TILs typically confer prognostic advantages, whereas the impact of CD4+ TILs is more variable, with Th1-skewed populations associated with prolonged survival [52]. Incorporating markers of TIL activation and effector function improves the accuracy of prognostic assessments. For instance, pre-existing PD-1+ CD8+ TILs predict better responses to PD-1 inhibitors in melanoma [53]. Additional exhaustion markers such as TIM-3 and LAG-3 are under active investigation for their prognostic significance [52]. PD-1 and TIM-3 frequently co-occur during T cell exhaustion [54], and our data revealed TIM-3 expression

in TME cells. Expression of TIM-3 was largely similar across SCC subgroups, except for significantly lower levels in KEB-SCCs. This finding diverges from earlier work reporting higher TIM-3 expression in DEB-SCCs compared with primary SCCs [50]. As a member of the TIM family, TIM-3 is expressed on IFNγ-secreting CD4+ and CD8+ T cells [55] and identifies the most impaired subset of CD8+PD-1+ tumor-infiltrating lymphocytes [55]. A phase I/Ib study of anti-TIM-3 monotherapy or its combination with anti-PD-1 therapy provided evidence of clinical activity in advanced solid malignancies [56]. Substantial LAG-3 expression was noted in the TME of nearly all SCCs, reaching the highest intensity in IS-SCCs. Increased LAG-3, often coexpressed with PD-L1, has been reported in advanced cutaneous SCCs [57]. As a member of the immunoglobulin superfamily, LAG-3 modulates T cell biology in diverse ways [40, 58]. It engages MHC-II on antigen-presenting cells and is displayed on TIL surfaces, contributing to T cell exhaustion [40]. LAG-3 blockade has proven effective in melanoma, particularly when paired with PD-1 inhibition [59, 60].

Collectively, these data highlight that EB-SCCs possess unique immune marker signatures distinct from those of IC- and IS-SCCs. DEB-SCCs and KEB-SCCs differed further, potentially reflecting the lack of chronic wounding in KEB and the multifaceted functions of kindlin-1.

Although reduced TIL infiltration, limited differentiation, and lower tumor mutational burden (TMB) likely drive the aggressive phenotype of EB-SCCs, the strong expression of PD-L1, IDO, and PD-1 in tumor cells and the surrounding TME identifies actionable therapeutic vulnerabilities. Strategies combining IDO inhibitors or IDO vaccination with PD-1 blockade may improve therapeutic responses. TIM-3 and LAG-3 inhibitors offer additional options for pairing with PD-1-targeted agents, while emerging bispecific antibodies have shown encouraging antitumor effects [61-63]. When integrated with our recent case reports [64], the present results enhance the immunological profiling of advanced cutaneous SCCs in EB and support the design of mechanistically informed treatments.

Conclusion

This study reveals that EB-SCCs exhibit distinct immune marker expression patterns and TIL densities relative to IC- and IS-SCCs. These observations advance immunological understanding of advanced cutaneous SCCs in EB patients and aid in selecting biologically tailored therapies when intervention is required.

Acknowledgments: None

Conflict of Interest: None

Financial Support: None

Ethics Statement: None

References

1. Fine JD, Johnson LB, Weiner M, Li KP, Suchindran C, et al. Epidermolysis Bullosa and the Risk of Life-Threatening Cancers: The National EB Registry Experience, 1986–2006. J Am Acad Dermatol. 2009;60:203-11.
2. Montaudié H, Chiaverini C, Sbidian E, Charlesworth A, Lacour JP, et al. Inherited Epidermolysis Bullosa and Squamous Cell Carcinoma: A Systematic Review of 117 Cases. Orphanet J Rare Dis. 2016;11:117.
3. Mallipeddi R. Epidermolysis Bullosa and Cancer. Clin Exp Dermatol. 2002;27:616-23.
4. Mellerio JE, Robertson SJ, Bernardis C, Diem A, Fine JD, George R, et al. Management of Cutaneous Squamous Cell Carcinoma in Patients with Epidermolysis Bullosa: Best Clinical Practice Guidelines. Br J Dermatol. 2016;174:56-67.
5. Yuen WY, Jonkman MF. Risk of Squamous Cell Carcinoma in Junctional Epidermolysis Bullosa, Non-Herlitz Type: Report of 7 Cases and a Review of the Literature. J Am Acad Dermatol. 2011;65:780-9.
6. Guerrero-Aspizua S, Conti CJ, Escamez MJ, Castiglia D, Zambruno G, Youssefian L, et al. Assessment of the Risk and Characterization of Non-Melanoma Skin Cancer in Kindler Syndrome: Study of a Series of 91 Patients. Orphanet J Rare Dis. 2019;14:183.
7. Harrs C, van den Akker PC, Baardman R, Duipmans JC, Horváth B, van Kester MS, et al. The Aggressive Behaviour of Squamous Cell Carcinoma in Epidermolysis Bullosa: Analysis of Clinical Outcomes and Tumour Characteristics in the Dutch EB Registry. Br J Dermatol. 2022;187:824-6.

8. Robertson SJ, Orrin E, Lakhan MK, O'Sullivan G, Felton J, Robson A, et al. Cutaneous Squamous Cell Carcinoma in Epidermolysis Bullosa: A 28-Year Retrospective Study. Acta Derm Venereol. 2021;101:adv00523.
9. Saleva M, Has C, He Y, Vassileva S, Balabanova M, Miteva L. Natural History of Kindler Syndrome and Propensity for Skin Cancer—Case Report and Literature Review. J Dtsch Dermatol Ges. 2018;16:338-41.
10. Shivaswamy KN, Sumathy TK, Shyamprasad AL, Ranganathan C. Squamous Cell Carcinoma Complicating Epidermolysis Bullosa in a 6-Year-Old Girl. Int J Dermatol. 2009;48:731-3.
11. Arnold AW, Bruckner-Tuderman L, Zuger C, Itin PH. Cetuximab Therapy of Metastasizing Cutaneous Squamous Cell Carcinoma in a Patient with Severe Recessive Dystrophic Epidermolysis Bullosa. Dermatology. 2009;219:80-3.
12. Medek K, Koelblinger P, Koller J, Diem A, Ude-Schoder K, Bauer JW, et al. Wundheilungsstörungen Während Der Antitumorösen Therapie Mit Cetuximab Bei Schwerer Generalisierter Dystropher Epidermolysis Bullosa. J Dtsch Dermatol Ges. 2019;17:448-50.
13. Diociaiuti A, Steinke H, Nyström A, Schwieger-Briel A, Meiss F, Pfannenberg C, et al. EGFR Inhibition for Metastasized Cutaneous Squamous Cell Carcinoma in Dystrophic Epidermolysis Bullosa. Orphanet J Rare Dis. 2019;14:278.
14. Kim M, Li M, Intong LR, Tran K, Melbourne W, Marucci D, et al. Use of Cetuximab as an Adjuvant Agent to Radiotherapy and Surgery in Recessive Dystrophic Epidermolysis Bullosa with Squamous Cell Carcinoma. Br J Dermatol. 2013;169:208-10.
15. Reimer A, Lu S, He Y, Bruckner-Tuderman L, Technau-Hafsi K, Meiss F, et al. Combined Anti-Inflammatory and Low Dose Antiproliferative Therapy for Squamous Cell Carcinomas in Recessive Dystrophic Epidermolysis Bullosa. J Eur Acad Dermatol Venereol. 2019;34:E1-E3.
16. Piccerillo A, El Hachem M, De Vito R, De Luca EV, Peris K, et al. Pembrolizumab for Treatment of a Patient with Multiple Cutaneous Squamous Cell Carcinomas and Recessive Dystrophic Epidermolysis Bullosa. JAMA Dermatol. 2020;156:708-10.
17. Duong T, Wong D, Barrett A, Price H. Successful Use of Immunotherapy to Treat Advanced Cutaneous Squamous Cell Carcinoma in Recessive Dystrophic Epidermolysis Bullosa. BMJ Case Rep. 2021;14:e238966.
18. Khaddour K, Gorell ES, Dehdashti F, Tang JY, Ansstas G, et al. Induced Remission of Metastatic Squamous Cell Carcinoma with an Immune Checkpoint Inhibitor in a Patient with Recessive Dystrophic Epidermolysis Bullosa. Case Rep Oncol. 2020;13:911-5.
19. Vasilev P, Kalev D, Karamanliev M, Dimitrov D, Troyanova P, Yordanova I. Cemiplimab Treatment of Squamous Cell Carcinoma in a Patient with Severe Recessive Dystrophic Epidermolysis Bullosa. J Dtsch Dermatol Ges. 2023;21:295-7.
20. Cho RJ, Alexandrov LB, den Breems NY, Atanasova VS, Farshchian M, Purdom E, et al. APOBEC Mutation Drives Early-Onset Squamous Cell Carcinomas in Recessive Dystrophic Epidermolysis Bullosa. Sci Transl Med. 2018;10:eaas9668.
21. Emmert H, Culley J, Brunton VG. Inhibition of Cyclin-Dependent Kinase Activity Exacerbates H2O2 -Induced DNA Damage in Kindler Syndrome Keratinocytes. Exp Dermatol. 2019;28:1074-8.
22. Sun Z, Costell M, Fässler R. Integrin Activation by Talin, Kindlin and Mechanical Forces. Nat Cell Biol. 2019;21:25-31.
23. Plow EF, Das M, Bialkowska K, Sossey-Alaoui K. Of Kindlins and Cancer. Discoveries. 2016;4:e59.
24. Wang P, Zhan J, Song J, Wang Y, Fang W, Liu Z, et al. Differential Expression of Kindlin-1 and Kindlin-2 Correlates with Esophageal Cancer Progression and Epidemiology. Sci China Life Sci. 2017;60:1214-22.
25. Kong J, Du J, Wang Y, Yang M, Gao J, Wei X, et al. Focal Adhesion Molecule Kindlin-1 Mediates Activation of TGF-β Signaling by Interacting with TGF-BRI, SARA and Smad3 in Colorectal Cancer Cells. Oncotarget. 2016;7:76224-37.
26. Fritsch A, Loeckermann S, Kern JS, Braun A, Bosl MR, Bley TA, et al. A Hypomorphic Mouse Model of Dystrophic Epidermolysis Bullosa Reveals Mechanisms of Disease and Response to Fibroblast Therapy. J Clin Investig. 2008;118:1669-79.
27. Heinemann A, He Y, Zimina E, Boerries M, Busch H, Chmel N, et al. Induction of Phenotype Modifying Cytokines by FERMT1 Mutations. Hum Mutat. 2011;32:397-406.

28. Chacón-Solano E, Leon C, Díaz F, García-García F, García M, Escámez MJ, et al. Fibroblast Activation and Abnormal Extracellular Matrix Remodelling as Common Hallmarks in Three Cancer-Prone Genodermatoses. Br J Dermatol. 2019;181:512-22.
29. Mittapalli VR, Madl J, Löffek S, Kiritsi D, Kern JS, Römer W, et al. Injury-Driven Stiffening of the Dermis Expedites Skin Carcinoma Progression. Cancer Res. 2016;76:940-51.
30. Ng YZ, Pourreyron C, Salas-Alanis JC, Dayal JHS, Cepeda-Valdes R, Yan W, et al. Fibroblast-Derived Dermal Matrix Drives Development of Aggressive Cutaneous Squamous Cell Carcinoma in Patients with Recessive Dystrophic Epidermolysis Bullosa. Cancer Res. 2012;72:3522-34.
31. Martins VL, Vyas JJ, Chen M, Purdie K, Mein CA, South AP, et al. Increased Invasive Behaviour in Cutaneous Squamous Cell Carcinoma with Loss of Basement-Membrane Type VII Collagen. J Cell Sci. 2009;122:1788-99.
32. Dayal JHS, Mason SM, Salas-Alanis JC, McGrath JA, Taylor RG, Mellerio JE, et al. Heterogeneous Addiction to Transforming Growth Factor-Beta Signalling in Recessive Dystrophic Epidermolysis Bullosa-Associated Cutaneous Squamous Cell Carcinoma. Br J Dermatol. 2020;184:697-708.
33. Hoste E, Arwert EN, Lal R, South AP, Salas-Alanis JC, Murrell DF, et al. Innate Sensing of Microbial Products Promotes Wound-Induced Skin Cancer. Nat Commun. 2015;6:5932.
34. Alexeev V, Huitema L, Phillips T, Cepeda R, de Los Cobos D, Perez RIM, et al. T-Cell Activation and Bacterial Infection in Skin Wounds of Recessive Dystrophic Epidermolysis Bullosa Patients. Exp Dermatol. 2022;31:1431-42.
35. Fife BT, Pauken KE. The Role of the PD-1 Pathway in Autoimmunity and Peripheral Tolerance. Ann N Y Acad Sci. 2011;1217:45-59.
36. Migden MR, Rischin D, Schmults CD, Guminski A, Hauschild A, Lewis KD, et al. PD-1 Blockade with Cemiplimab in Advanced Cutaneous Squamous-Cell Carcinoma. N Engl J Med. 2018;379:341-51.
37. Curran TA, Jalili RB, Farrokhi A, Ghahary A. IDO Expressing Fibroblasts Promote the Expansion of Antigen Specific Regulatory T Cells. Immunobiology. 2014;219:17-24.
38. Holmgaard RB, Zamarin D, Li Y, Gasmi B, Munn DH, Allison JP, et al. Tumor-Expressed IDO Recruits and Activates MDSCs in a Treg-Dependent Manner. Cell Rep. 2015;13:412-24.
39. Das M, Zhu C, Kuchroo VK. Tim-3 and Its Role in Regulating Anti-Tumor Immunity. Immunol Rev. 2017;276:97-111.
40. Long L, Zhang X, Chen F, Pan Q, Phiphatwatchara P, Zeng Y, et al. The Promising Immune Checkpoint LAG-3: From Tumor Microenvironment to Cancer Immunotherapy. Genes Cancer. 2018;9:176-89.
41. Bankhead P, Loughrey MB, Fernández JA, Dombrowski Y, McArt DG, Dunne PD, et al. QuPath: Open Source Software for Digital Pathology Image Analysis. Sci Rep. 2017;7:16878.
42. Stratigos A, Garbe C, Lebbe C, Malvehy J, del Marmol V, Pehamberger H, et al. Diagnosis and Treatment of Invasive Squamous Cell Carcinoma of the Skin: European Consensus-Based Interdisciplinary Guideline. Eur J Cancer. 2015;51:1989-2007.
43. Föll MC, Fahrner M, Gretzmeier C, Thoma K, Biniossek ML, Kiritsi D, et al. Identification of Tissue Damage, Extracellular Matrix Remodeling and Bacterial Challenge as Common Mechanisms Associated with High-Risk Cutaneous Squamous Cell Carcinomas. Matrix Biol. 2018;66:1-21.
44. Nyström A, Bruckner-Tuderman L, Kiritsi D. Dystrophic Epidermolysis Bullosa: Secondary Disease Mechanisms and Disease Modifiers. Front Genet. 2021;12:737272.
45. Mittapalli VR, Kühl T, Kuzet SE, Gretzmeier C, Kiritsi D, Gaggioli C, et al. STAT3 Targeting in Dystrophic Epidermolysis Bullosa. Br J Dermatol. 2020;182:1279-81.
46. Haghighi Javid A, Li D, Technau-Hafsi K, Has C. Interleukin-17A Immune Pattern across Genetic Acantholytic and Blistering Disorders. Clin Exp Dermatol. 2023;48:518-23.
47. Annicchiarico G, Morgese MG, Esposito S, Lopalco G, Lattarulo M, Tampoia M, et al. Proinflammatory Cytokines and Antiskin Autoantibodies in Patients with Inherited Epidermolysis Bullosa. Medicine. 2015;94:e1528.
48. Zakharia Y, McWilliams RR, Rixe O, Drabick J, Shaheen MF, Grossmann KF, et al. Phase II Trial of the IDO Pathway Inhibitor Indoximod plus Pembrolizumab for the Treatment of Patients with Advanced Melanoma. J Immunother Cancer. 2021;9:e002057.

49. Kjeldsen JW, Lorentzen CL, Martinenaite E, Ellebaek E, Donia M, Holmstroem RB, et al. A Phase 1/2 Trial of an Immune-Modulatory Vaccine against IDO/PD-L1 in Combination with Nivolumab in Metastatic Melanoma. Nat Med. 2021;27:2212-23.
50. Filoni A, Cicco G, Cazzato G, Bosco A, Lospalluti L, Tucci M, et al. Immune Disregulation in Cutaneous Squamous Cell Carcinoma of Patients with Recessive Dystrophic Epidermolysis Bullosa: A Single Pilot Study. Life. 2022;12:213.
51. Filoni A, Cicco G, Lospalluti L, Maglietta A, Foti C, Annichiarico G, et al. Morphological and Morphometric Analysis of Cutaneous Squamous Cell Carcinoma in Patients with Recessive Dystrophic Epidermolysis Bullosa: A Retrospective Study. J Eur Acad Dermatol Venereol. 2020;34:1707-14.
52. Brummel K, Eerkens AL, de Bruyn M, Nijman HW. Tumour-Infiltrating Lymphocytes: From Prognosis to Treatment Selection. Br J Cancer. 2023;128:451-8.
53. Tumeh PC, Harview CL, Yearley JH, Shintaku IP, Taylor EJM, Robert L, et al. PD-1 Blockade Induces Responses by Inhibiting Adaptive Immune Resistance. Nature. 2014;515:568-71.
54. Li J, Ferris RL. Differential Expression of PD-1 and Tim-3 Marks Activation versus Exhaustion Status of T Cells in the Tumor Microenvironment. J ImmunoTher Cancer. 2014;2:P220.
55. Wolf Y, Anderson AC, Kuchroo VK. TIM3 Comes of Age as an Inhibitory Receptor. Nat Rev Immunol. 2020;20:173-85.
56. Curigliano G, Gelderblom H, Mach N, Doi T, Tai D, Forde PM, et al. Phase I/Ib Clinical Trial of Sabatolimab, an Anti-TIM-3 Antibody, Alone and in Combination with Spartalizumab, an Anti-PD-1 Antibody, in Advanced Solid Tumors. Clin Cancer Res. 2021;27:3620-9.
57. Wu S, Slater NA, Sayed CJ, Googe PB. PD-L1 and LAG-3 Expression in Advanced Cutaneous Squamous Cell Carcinomas. J Cutan Pathol. 2020;47:882-7.
58. He Y, Rivard CJ, Rozeboom L, Yu H, Ellison K, Kowalewski A, et al. Lymphocyte-Activation Gene-3, an Important Immune Checkpoint in Cancer. Cancer Sci. 2016;107:1193-7.
59. Tawbi HA, Schadendorf D, Lipson EJ, Ascierto PA, Matamala L, Castillo Gutiérrez E, et al. Relatlimab and Nivolumab versus Nivolumab in Untreated Advanced Melanoma. N Engl J Med. 2022;386:24-34.
60. Amaria RN, Postow M, Burton EM, Tezlaff MT, Ross MI, Torres-Cabala C, et al. Neoadjuvant Relatlimab and Nivolumab in Resectable Melanoma. Nature. 2022;611:155-60.
61. Liu J, Luan Y, Deng H, Wang F, Wang C, Zhang Z. A Bivalent Tim-3/PD-1 Bispecific Antibody for the Treatment of PD-1 Antibody Resistant or Refractory NSCLC. J Clin Oncol. 2022;40:e14597.
62. Sung E, Ko M, Won J, Jo Y, Park E, Kim H, et al. LAG-3xPD-L1 Bispecific Antibody Potentiates Antitumor Responses of T Cells through Dendritic Cell Activation. Mol Ther. 2022;30:2800-16.
63. Shi N, Zhou Y, Liu Y, Zhang R, Jiang X, Ren C, et al. PD-1/LAG-3 Bispecific Antibody Potentiates T Cell Activation and Increases Antitumor Efficacy. Front Immunol. 2022;13:1047610.
64. Trefzer L, Hess ME, Scholten L, Technau-Hafsi K, Meiss F, Boerries M, et al. Variable Outcome of Immunotherapy in Advanced Multiple Cutaneous Squamous Cell Carcinomas in Two Patients with Recessive Dystrophic Epidermolysis Bullosa. Acta Dermatovenerol. 2023;103:4870.